



# Determination of Five Organochlorine Pesticides Based on GC–MS Coupled with Deep Eutectic Solvent-Modified Magnetic Graphene Oxide-Improved QuEChERS in Vegetables

Ling Yu<sup>1</sup> · Shujiao Zhang<sup>1</sup> · Xu He<sup>1</sup> · Jie Hu<sup>1</sup> · Zhiju Zhao<sup>1</sup> · Aiqing Xia<sup>1</sup> · Cuijuan Xing<sup>1</sup> · Ruibing Zhao<sup>1</sup> · Jiawei Zhang<sup>1</sup>

Received: 5 April 2023 / Revised: 31 May 2023 / Accepted: 5 June 2023 / Published online: 28 June 2023  
© The Author(s), under exclusive licence to Springer-Verlag GmbH Germany, part of Springer Nature 2023

## Abstract

A novel deep eutectic solvent-modified magnetic graphene oxide (DES@MGO) was first synthesized. The microscopic structure, composition, and property of the new magnetic adsorbent was characterized. QuChERS-based DES@MGO was first investigated for the removal of impurities from vegetables. Various influencing factors, such as extraction solvent, the mass of anhydrous  $\text{MgSO}_4$ , the mass of adsorbent, and the oscillation time, had been systematically tested. The linearity of the method for analysis of  $\alpha$ -HCH,  $\beta$ -HCH,  $\delta$ -HCH, and p,p'-DDE was between the range of 5–100  $\mu\text{g kg}^{-1}$ , and for analysis of  $\gamma$ -HCH was 10–100  $\mu\text{g kg}^{-1}$ . The limits of detection, the limits of quantification, and correlation coefficients were 0.3–2.0  $\mu\text{g kg}^{-1}$ , 0.9–6.6  $\mu\text{g kg}^{-1}$ , and 0.9986–0.9997, respectively. In comparison to the traditional purification materials *N*-propylethylenediamine (PSA) and magnetic graphene oxide (MGO), DES@MGO exhibited superior adsorbent properties and purification performance with more fast adsorption rate, and could effectively remove the majority interfering substances in vegetable extract with achieving good retention of the 5 organochlorine pesticides (OCPs). In the meantime, as a pretreatment material, the DES@MGO showed the advantage of rapid separation with its favorable magnetism. Herein, the method is of easy operation and accurate quantification, which is suitable for the analysis of OCPs in vegetables.

**Keywords** Deep eutectic solvent-modified magnetic graphene oxide · QuEChERS · Gas chromatography–mass spectrometry · Organochlorine

## Introduction

Organochlorine pesticides (OCPs) have been deemed as one class of compounds that despite their good biological activity and environmental compatibility may produce a range of toxic side effects. It was widely used in the 1960 of the twentieth century. OCPs played an important role in controlling agricultural pests and diseases, increasing agricultural production and farmers' incomes. However, OCPs are a typical highly toxic, persistent, and highly bioaccumulative organic pollutants, which pose potential hazards to the environment and human health [1]. Thus, from 1970 to 1980,

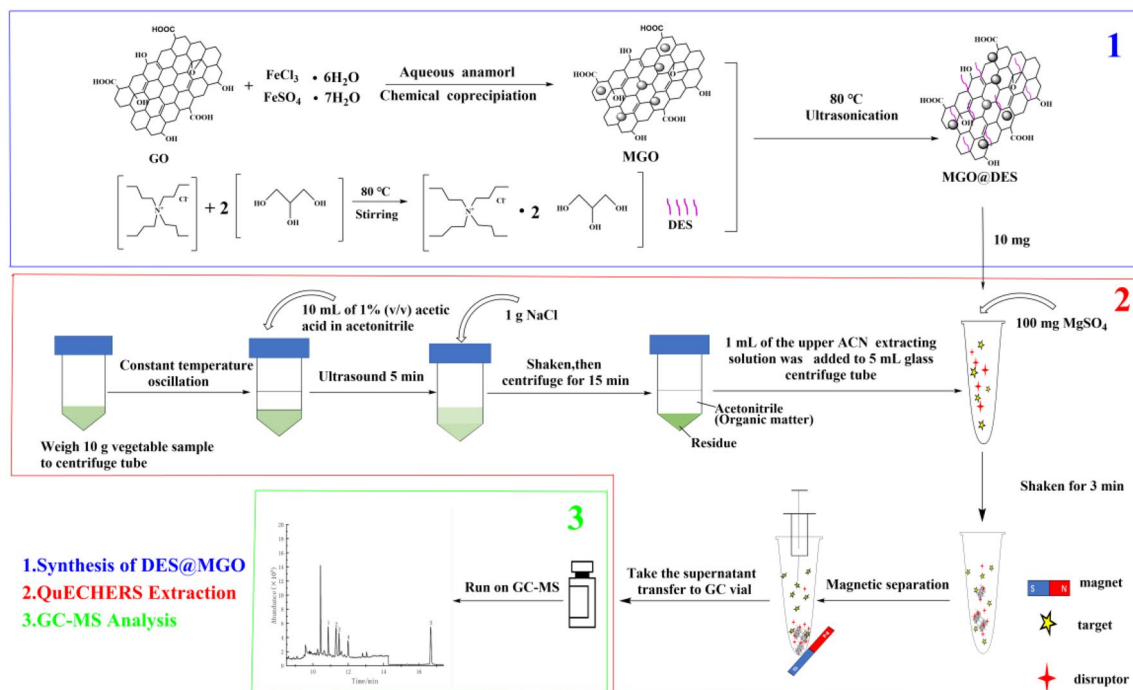
OCPs have been banned in many countries for public health and environmental reasons. However, OCPs have been continuously enriched in the environmental medium due to the previously vast using amount. It aroused huge attention due to OCP's toxicity, carcinogenicity, and biomagnification through the food chain [2]. It is widely known that the vegetables have essential components for a healthy diet which contain amounts of nutrients and minerals, while unfortunately OCPs still have high detection rates in these kinds of environmental media [3–5] or foods [6, 7]. Therefore, it is urgent to study the detection methods of accurate, rapid, and sensitive OCPs in vegetables.

QuEChERS is the acronym for Quick, Easy, Cheap, Rugged, and Safe, which has been widely used in food analysis [8–10] and environmental analysis [11, 12] mainly attribute to its high versatility. QuEChERS contains two parts: the extraction and clean-up steps. Especially, the clean-up step plays a vital role in the QuEChERS process, and the choice of the clean-up materials is of a decisive significance. The traditional clean-up materials contain primary secondary

✉ Ling Yu  
44427364@qq.com

✉ Shujiao Zhang  
285304264@qq.com

<sup>1</sup> College of Chemistry and Chemical Engineering, Xingtai University, Xingtai 054001, China



**Scheme 1** Synthesis of DES@MGO and determination of OCPs by QuEChERS

amine (PSA), graphitized carbon black (GCB), and octadecyl modified silica (C18) which are also combined-used, and the performance is unsatisfactory for the treatment of complex matrix samples. To solve the problems, researchers have focused on developing high-efficiency clean-up materials such as magnetic fluorinated multi-walled carbon nanotubes (M-F-MWCNTs) [13],  $\text{Fe}_3\text{O}_4$  magnetic nanoparticles [14], amine-functional reduced graphene oxide [15], and magnetic graphene oxide (MGO) [16]. Particularly, the MGO has attracted extraordinary research interest.

Graphene oxide (GO) is an oxidized form of graphene, which belongs to the amphiphilic flexible two-dimensional material, and endows a large surface areas due to the layered fold structures [17]. Moreover, abundant hydrophilic oxygen-containing functional groups ( $-\text{O}-$ ,  $-\text{OH}$  and  $-\text{COOH}$ , etc.) at the basal plane or sheet edge of GO could effectively enhance the dispersion of GO in solvents, facilitating the interaction of GO with the target analytes through hydrogen bonding,  $\pi-\pi$ , and electrostatic interactions. Thus, it has been regarded as an ideal clean-up material for QuEChERS.

However, since the adsorption process of GO is usually carried out in solution, it encounters the problem of separation of GO from the treated solution. Traditional separation methods, such as centrifugation and filtration, are cumbersome and time-consuming, resulting higher costs in practical applications. By comparison, separation via using functional materials showed much more advantage. Magnetic nanoparticles ( $\text{Fe}_3\text{O}_4$ ) have been widely used for rapid separation due

to their strong superparamagnetism. Hence, introduction of the magnetic  $\text{Fe}_3\text{O}_4$  into GO might be propitious to enhance solid-liquid separation, realizing the effective combination of purification and magnetic separation.

Recently, deep eutectic solvent (DES) has also been attracting much attention as a new generation of green solvents [19]. DES is a eutectic mixture formed by self-association of hydrogen-bond donors (HBD) and hydrogen-bond acceptor (HBA). It has excellent properties such as being easier to synthesize, low cost, less toxic, and biodegradability. Thus, DESs play a key role and act as new, efficient green solvents [20]. The DES and MGO could be combined through hydrogen bonding and electrostatic interaction, providing more abundant functional groups on the surface of the DES@MGO and promoting the dispersion of MGO in polar solvents. Vegetable matrix is complex and contains a lot of organic matters. Theoretically, the abundant functional groups in DES@MGO have a strong adsorption effect on the vegetable matrix through dipolar-dipole interaction, hydrophobic interaction, and  $\Pi-\Pi$  accumulation. Therefore, it could be reasonably deduced that DES@MGO might be an effective clean-up material for the QuEChERS application on the vegetable.

Herein, in this paper, a new material of DES@MGO with MGO as the support and a DES synthesized by tetrabutylammonium chloride-glycerol as the functional monomer was successfully synthesized. The DES@MGO was used as a clean-up material for QuEChERS.

Subsequently, OCPs in vegetables were detected by the Gas Chromatography–Mass Spectrometer (GC–MS) (Scheme 1). The synthesized DES@MGO was characterized via TEM, XRD, FTIR, VSM, TGA, and BET. By optimizing the extraction solvent, the mass of anhydrous  $\text{MgSO}_4$ , the mass of adsorbent and the oscillation time, and the optimal pretreatment conditions for QuEChERS were established and the methodology was verified. What's more, the DES@MGO exhibited highly accurate and rapid purification of OCPs in vegetable samples with the established method in comparison to the conventional sorbent PSA and MGO. The introduction of DES in the synthesis of graphene was of great significance for developing the green synthesis of new functional carbon materials and providing useful guidance in the field of pesticide residue detection and analysis.

## Materials and Methods

### Instruments and Reagents

GC/MS-QP 2010 Ultra (Shimadzu Corporation, Japan), SC-3612 centrifuge (Anhui Zhongke Zhongjia Scientific Instrument Co., LTD., China), KQ-50E Ultrasonic Cleaner (Kunshan Ultrasonic Instrument Co., LTD., China), Milli-Q Ultrapure water apparatus (Millipore Corporation, USA), JEM 2100(magnetic) and JEM 2800 (non-magnetic) Transmission Electron Microscope (TEM, JEOL, Japan), XRD-6100 X-ray Diffraction (XRD, Shimadzu, Japan), Nicolet iS20 FTIR Spectrometer (FTIR, Thermo Scientific, USA), 7404 Vibrating Sample Magnetometer (VSM, LakeShore, USA), TG/DTA8122 Thermal Gravimetric Analyzer (TGA, Rigaku, Japan), and ASAP 2460 Automatic Surface and Porosity Analyzer (BET, Micromeritics, USA).

OCPs standards ( $50 \mu\text{g kg}^{-1}$ ) of  $\alpha$ -,  $\beta$ -,  $\gamma$ -,  $\delta$ - hexachlorocyclohexanes (HCH) and *p,p'*-DDE ([2,2-bis(*p*-chlorophenyl)-1,1-dichloroethylene]) were gained from China Institute of metrology (Beijing, China). HPLC-grade methanol was from Fisher Scientific (New Jersey, USA). Primary secondary amine (PSA) with average particle diameter 40–60  $\mu\text{m}$  was obtained from Weiqiboxing Biotechnology Co. Ltd. (Wuhan, China). The graphitized carbon black (GCB) was purchased from Biosun Company (Japan). The anhydrous magnesium sulfate ( $\text{MgSO}_4$ ), concentrated sulfuric acid ( $\text{H}_2\text{SO}_4$ ), and graphite powder were purchased from Hedong District of Tianjin Hongyan Reagent Factory (Tianjin, China). Acetonitrile, glacial acetic acid, sodium chloride, potassium nitrate, potassium permanganate, hydrogen peroxide,  $\text{FeCl}_3 \cdot 6\text{H}_2\text{O}$ ,  $\text{FeSO}_4 \cdot 7\text{H}_2\text{O}$ , tetrabutylammonium chloride, and glycerol

were all analytically pure, gained from Tianjin Yongda Chemical Reagent Co. Ltd. (Tianjin, China).

### Preparation of Standard Solution

The single standard solution at  $50 \mu\text{g mL}^{-1}$  was prepared in HPLC-grade methanol to prepare a mixed standard solution with a concentration of  $1 \mu\text{g mL}^{-1}$ .

Appropriate amount of single standard solution was diluted into series of standard working solutions of 5, 10, 25, 50, 75, and  $100 \mu\text{g L}^{-1}$  with HPLC-grade methanol to calculate the recoveries after QuEChERS. All the standard solutions were stored at  $4^\circ\text{C}$ .

### Synthesis of GO

GO was synthesized and modified according to the reported literature [21]. First, 120 mL  $\text{H}_2\text{SO}_4$  was placed under an ice-water bath. After that 4 g of graphite powder and 2 g  $\text{KNO}_3$  were added. When the reaction lasted for 30 min, 12 g  $\text{KMnO}_4$  was added. The reaction was continued to stirring for other 2 h. The whole process was completely carried out under the condition of ice-water bath. Afterward, the solution was kept stirring at  $40^\circ\text{C}$  for other 24 h. And then, 400 mL of ultra-pure water was added. After that, 20 mL  $\text{H}_2\text{O}_2$  (30%) was added to the solution until it turned bright yellow and no air bubbles were formed. The obtained product was washed with ultra-pure water and ethanol till it reached neutral pH. Finally, it was dried in a vacuum oven.

### Synthesis of MGO

The MGO composite was synthesized by improved chemical coprecipitation method [16]. First, ultra-sonicated the 200 mL of GO solution ( $3.0 \text{ mg mL}^{-1}$ ) for 30 min. In addition, 6 g  $\text{FeCl}_3 \cdot 6\text{H}_2\text{O}$  and 3.3 g  $\text{FeSO}_4 \cdot 7\text{H}_2\text{O}$  were added into 200 mL ultra-pure water for 1.5 h to dissolve completely. Mix the two solutions, and then,  $\text{NH}_3 \cdot \text{H}_2\text{O}$  (27%, w/v) was added to adjust the pH value to 9. The experiment continued to ultrasonic for 2 h. Finally, separated the particles through a magnet. The product cleaned by  $\text{H}_2\text{O}$  until the pH value was 7 and then washed with methanol for three times. After washing, the product was vacuum dried and the MGO were gotten.

### Synthesis of DES@MGO

Synthesis of DES: 20 g tetrabutylammonium chloride and 10 mL glycerol (molar ratio 1:2) were stirred for 30 min at  $80^\circ\text{C}$ . A colorless and transparent homogeneous liquid was obtain.

Synthesis of DES@MGO: 1.5 g MGO was placed in a beaker, 6 mL DES was dissolved in 60 mL methanol and

added to beaker, and then stir well and ultrasonic for 2 h. Subsequently, the product was washed with methanol for several times and dried in vacuum.

### Sample Preparation

Four types of vegetables, such as cabbage, spinach, cucumbers, and tomatoes, were purchased from local supermarkets (Xingtai, China) for investigation. Samples were homogenized and stored at  $-18\text{ }^{\circ}\text{C}$  in glass containers.

### QuEChERS Step

10 g of homogenized vegetable samples were transferred into a 50 mL centrifuge tube and extracted for 10 min by oscillating in a constant temperature shaker. After that, 10 mL of 1% (v/v) acetic acid in acetonitrile was added and the tube was ultrasound for 5 min. Next, 1 g NaCl was added, and the tube was shaken for 1 min to prevent salt agglomeration. The mixture was centrifuged at 5000 rpm for 15 min. Then, 1 mL of the upper ACN extracting solution was added to 5 mL glass centrifuge tube. Subsequently, 10 mg DES@MGO and 100 mg anhydrous  $\text{MgSO}_4$  were added. Successively, the mixture was violently shaken for 3 min. An external magnetic field was used for the separation of the adsorbents from the solution. Finally, 1  $\mu\text{L}$  was injected into the GC/MS for analysis.

### Chromatographic Conditions

The GC was fitted with an Rxi-5silMS column ( $30\text{ m}\times 0.25\text{ mm}\times 0.25\text{ }\mu\text{m}$ ) (Shimadzu, Japan). Helium was used as the carrier gas at a flow rate of  $1\text{ mL}\cdot\text{min}^{-1}$  (purity  $\geq 99.999\%$ ). The inlet temperature was  $250\text{ }^{\circ}\text{C}$ . The sample with size of  $1.0\text{ }\mu\text{L}$  was injected in the splitless mode. Temperature procedure: the initial temperature was set as  $50\text{ }^{\circ}\text{C}$  and maintained for 1 min, then raised to  $200\text{ }^{\circ}\text{C}$  at  $20\text{ }^{\circ}\text{C}\text{ min}^{-1}$ , raised to  $230\text{ }^{\circ}\text{C}$  at  $5\text{ }^{\circ}\text{C}\text{ min}^{-1}$ , and maintained for 3 min.

### Mass spectrometry conditions

The mass spectrometer was operated in electron ionization mode at 70 eV. The ion source temperature and interface temperature were set as  $260\text{ }^{\circ}\text{C}$  and  $^{\circ}\text{C}$ , respectively. The solvent delay time was 5 min. Separation of the OCPs was sufficient to set up the full scan in the range 40–500  $m/z$  and selected ion monitoring (SIM) mode. The retention time, and qualitative and quantitative ions for the OCPs are listed in Table 1.

**Table 1** Retention time, and qualitative and quantitative ions of 5 OCPs

Peak number	Compound	Retention time (min)	Mass-to-charge ratio ( $m/z$ )	
			Quantitative ion	Qualitative ion
1	$\alpha$ -HCH	10.835	181	181,183,219
2	$\beta$ -HCH	11.260	109	109,181,183
3	$\gamma$ -HCH	11.450	181	181,183,219
4	$\delta$ -HCH	11.945	181	181,183,219
5	p,p'-DDE	16.625	246	246,248,318

### Matrix Effect (ME)

$\text{ME} = \frac{A_M - A_S}{A_S} \times 100\%$ , where  $A_M$  was the peak area of the object to be measured in the sample matrix, and  $A_S$  is the peak area of the object to be measured in pure solvent. Evaluation criteria:  $\text{ME} > 0$ , matrix enhancement;  $\text{ME} < 0$ , matrix inhibition; The matrix effect was not significant with the ME value between 0 and 25%. While the matrix effect became slightly significant when the ME value was between 25 and 50%. And it showed significant matrix effect when the ME was greater than 50%.

$$\text{Recovery}(\%) = \frac{C_2 - C_1}{C_0} \times 100$$

where  $C_1$  is measured concentration in unadded sample,  $C_2$  is measured concentration of target in added sample, and  $C_0$  is theoretical concentration of target in added sample.

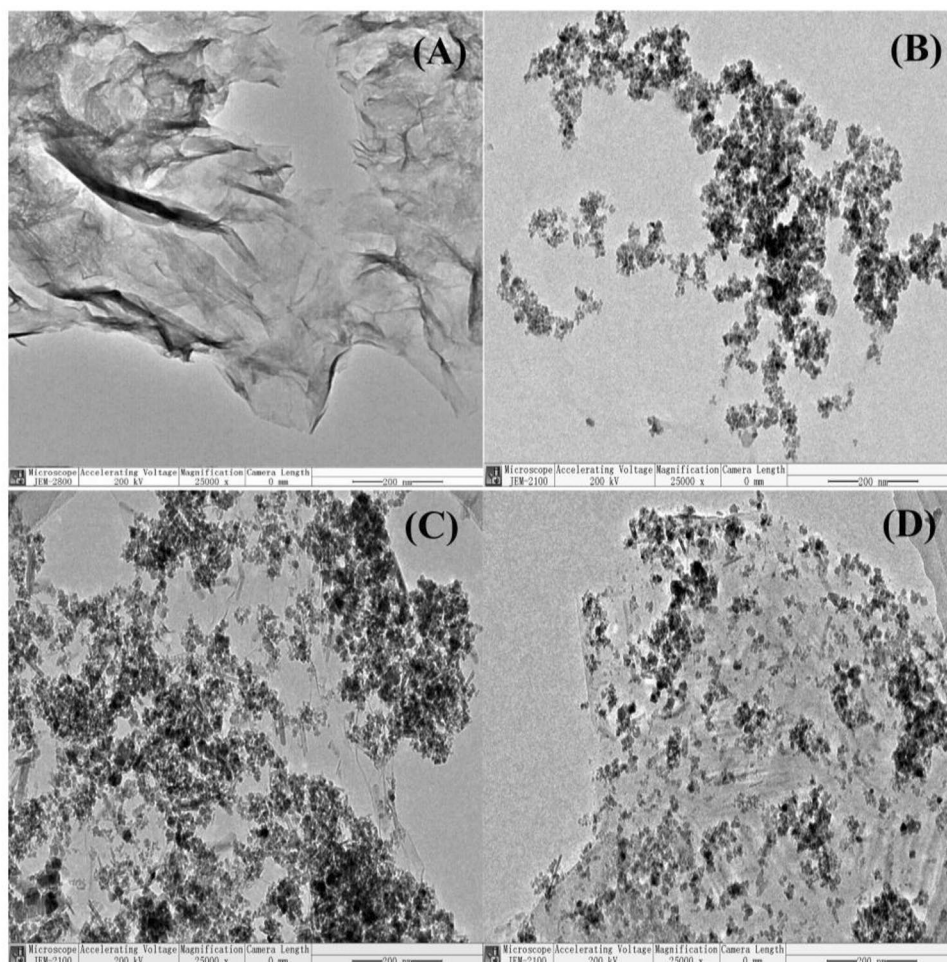
Experiments were repeated three times to validate the repeatability of the results. The results presented are the average of the three experiments conducted. Origin 2021 software is used as statistical treatment to reach the conclusion described in the work.

## Results and Discussion

### Characterization of DES@MGO

The morphology of GO,  $\text{Fe}_3\text{O}_4$ , MGO, and DES@MGO was investigated by the transmission electron microscopy (TEM) and the results are displayed in Fig. 1. As can be seen from Fig. 1A, GO presented as a translucent sheet structure with a smooth surface and some wrinkle structures, which is advantageous for enhancing its specific surface area and beneficial to the loading of magnetic nanoparticles, improving the adsorption performance [22]. As shown in Fig. 1B,

**Fig. 1** TEM images of GO (A), Fe<sub>3</sub>O<sub>4</sub> (B), MGO (C), and DES@MGO (D)



Fe<sub>3</sub>O<sub>4</sub> displayed as aggregated particle size with size ranging from 5 to 20 nm. From Fig. 1C, it can be seen the Fe<sub>3</sub>O<sub>4</sub> loaded at the surface of GO successfully and the particles were evenly dispersed, which inhibits Fe<sub>3</sub>O<sub>4</sub> agglomeration to a certain extent. After forming magnetic DES@MGO, it could be observed in Fig. 1D that the MGO was surrounded by a semitransparent liquid. It might be due to the DES. Meanwhile, the Fe<sub>3</sub>O<sub>4</sub> particles were more dispersed and uniform. The results of TEM also illustrated that the DES was modified on MGO.

The X-ray diffraction measurements were conducted on graphite, GO, Fe<sub>3</sub>O<sub>4</sub>, MGO, and DES@MGO (diffraction angles ranging from 5 to 80°), and the results are shown in Fig. 2A. It can be seen in Fig. 2A that the diffraction peak at  $2\theta = 26.30^\circ$  could be ascribed to graphite. An obvious peak appeared at  $2\theta = 10.78^\circ$  can be attributed to the special layered structure of GO [23], indicating the successful synthesis of GO [24]. Six discernible diffraction peaks for Fe<sub>3</sub>O<sub>4</sub> shown clearly at  $2\theta = 30.08^\circ, 35.38^\circ, 43.04^\circ, 53.34^\circ, 57.02^\circ,$  and  $62.64^\circ$  belonged to the (220), (311), (400), (422), (511), and (440) planes, respectively [25]. These six peaks were also presented in diffraction pattern of MGO, indicating

that Fe<sub>3</sub>O<sub>4</sub> has been successfully modified on the GO and remained good crystal structure throughout the synthesis process. Nevertheless, the peak of GO was not observed in the diffraction pattern of MGO, which may be due to the reduction of the accumulation between GO lamellae caused by the ultrasonic treatment of GO and the introduction of magnetic Fe<sub>3</sub>O<sub>4</sub> in the preparation process, resulting in the reduction of the intensity of the carbon diffraction peak. By comparing diffraction pattern of MGO, the DES@MGO showed almost similar curves, which indicates that the DES successfully modified on MGO with retaining the crystal structure of MGO.

FTIR spectroscopy was used to examine the chemical compositions of GO, MGO, and DES@MGO according to Fig. 2B. It can be seen from the curve of GO that, the bands at  $3172\text{ cm}^{-1}, 1731\text{ cm}^{-1}, 1614\text{ cm}^{-1},$  and  $1223\text{ cm}^{-1}$  were assigned to the stretching vibration of O–H, C=O, C=C, and C–O. The peak at  $1050\text{ cm}^{-1}$  was attributed to the skeleton stretching vibration of C–O–C. In the curve of MGO, the peak at  $577\text{ cm}^{-1}$  was corresponding to the stretching vibration of Fe–O [26], indicating that Fe<sub>3</sub>O<sub>4</sub> has been successfully loaded on the GO surface, which was consistent

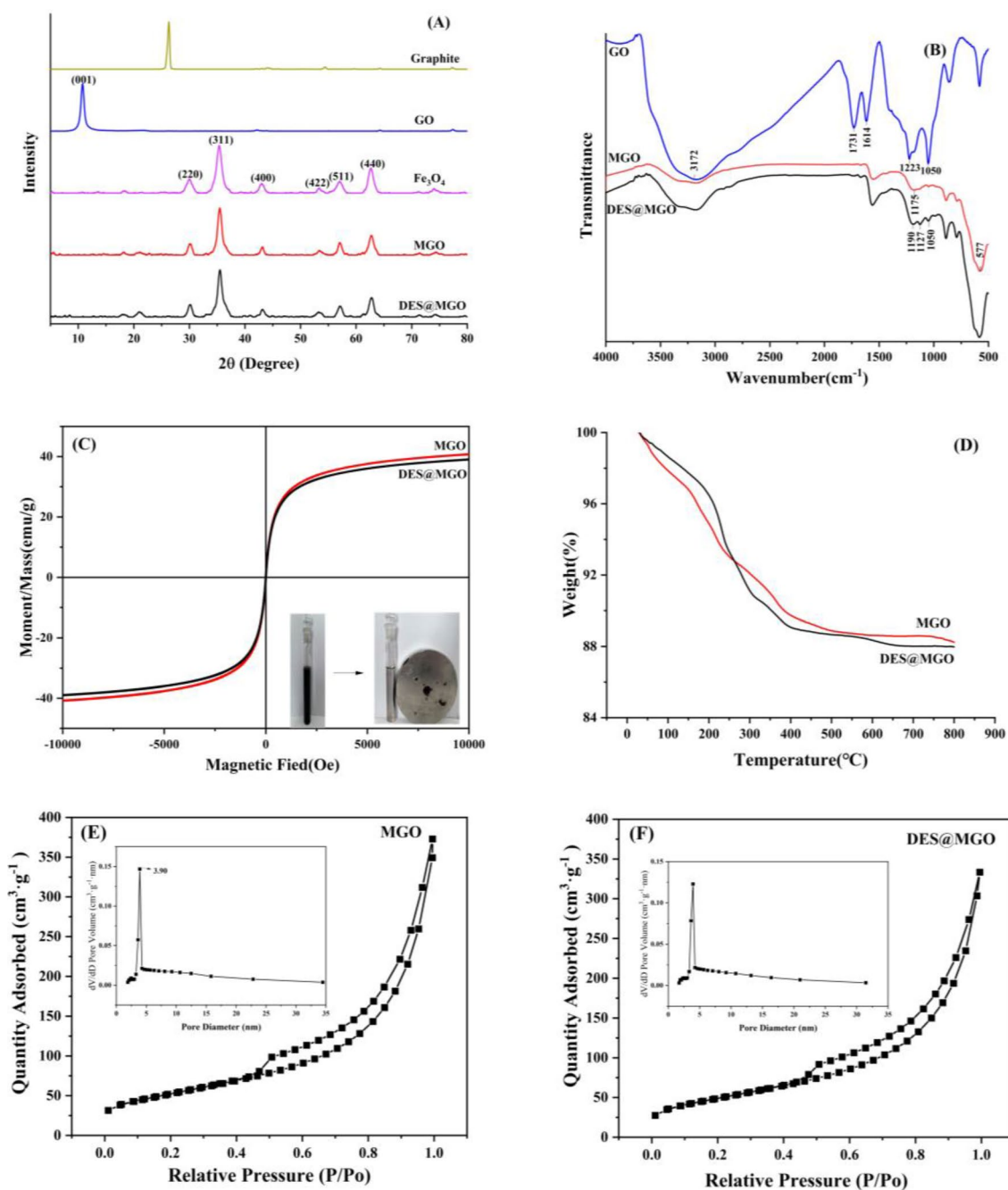


**Fig. 2** X-ray diffraction (A), FTIR spectra (B), magnetization curves (C), TGA curves (D), the  $N_2$  adsorption–desorption curves of MGO (E), and the  $N_2$  adsorption–desorption curves of DES@MGO (F)

with the results of the TEM and XRD. Moreover, most of the characteristic peaks were weakened after the introduction of  $Fe_3O_4$ . Compared with the curve of MGO, two new peaks of  $1127\text{ cm}^{-1}$  and  $1050\text{ cm}^{-1}$  appeared in the curve of DES@MGO, which might be ascribed to the stretching vibrations of C–O and C–N in tetrabutylammonium chloride. It was confirmed that DES was successfully modified on MGO.

The magnetic value is an important property parameter of magnetic separation of the extractant. The particles of MGO and DES@MGO were tested by a VSM (Fig. 2C). The hysteresis curves of MGO and DES@MGO were both S-shaped and superparamagnetic, without hysteresis phenomenon. The saturation magnetization of curve MGO and DES@MGO were  $43.05$  and  $41.09\text{ emu g}^{-1}$ , respectively. The magnetic saturation value of DES@MGO had a slight

decrease after DES was modified on the MGO, which may be because the modification of non-magnetic DES on the surface of MGO resulted in partial shielding of the MGO magnetic response. In addition, DES@MGO dispersed well in acetonitrile and easily separated by magnetic plate (seen from the inset of Fig. 2C).

The thermogravimetric analysis (TGA) of MGO and DES@MGO was investigated by thermal gravimetric analysis (shown in Fig. 2D). The experiment was measured from room temperature to 800 °C in argon atmosphere and the temperature changed by 10 K min<sup>-1</sup>. MGO and DES@MGO displayed similar trends and intersect at 260°C. The mass loss below 140 °C could be attributable to evaporation of the surface moisture material and crystalline water [27]. The weight loss of MGO and DES@MGO were 2.96% and 2.07%, respectively. The heat loss of MGO and DES@MGO between 140 and 400 °C was 7.3% and 8.85%, respectively, which might be due to the thermal decomposition of unstable functional groups on the GO surface [28]. The heat loss of the two materials between 400 and 550 °C could be attributed to the thermal decomposition of the stable oxygen-containing functional groups on the GO surface [28], which were 1.01% and 0.52%, respectively. When the temperatures were above 550 °C, DES@MGO showed a slight mass loss process, which may be related to the decomposition of its crosslinked structure. It might be explained by the thermal decomposition of DES in DES@MGO. Moreover, DES@MGO exhibited less mass loss and better thermal stability below 264 °C compared with that of the MGO.

The structural characteristics, such as adsorption–desorption isotherm, BET surface area, and average pore size and pore volume of MGO and DES@MGO, were investigated via the BET method (shown in Fig. 2E, F and Table 2). According to the IUPAC classification, the N<sub>2</sub> adsorption–desorption isotherms exhibited the type-IV isotherm [27]. In addition, hysteresis loops similar to H3 can be observed in the range of relative pressure ( $P/P_0$ ) of 0.44–1, indicating that the samples have lamellar mesoporous structure, which correspond to the TEM structure. As can be seen in Table 2, The BET-specific surface area of MGO and DES@MGO was determined to be 189.74 m<sup>2</sup> g<sup>-1</sup> and 178.89 m<sup>2</sup> g<sup>-1</sup>, respectively. And the surface area decreased slightly after DES modification on

MGO. Besides, the average pore diameter and pore volume of DES@MGO also decreased slightly in comparison to MGO, which may be caused by the modification of DES on the surface of MGO.

## QuEChERS Optimization

### Optimization of Extraction Solvent

Generally, vegetable samples contain a lot of water. According to the previous report [29], acetonitrile has been deemed as a general extraction solvent, and thus, acetonitrile was preliminary selected as an extraction solvent. The target pesticide should be sufficiently soluble and stable in the extraction solvent. The recoveries of all pesticides to be tested cannot be fully taken into account using a single solvent extraction. Considering the need for simultaneous detection of multiple pesticides and further improving the extraction efficiency of samples, five OCPs (50 µg kg<sup>-1</sup>) were added to the blank substrate of Chinese cabbage to carry out extraction experiments. The extraction effects of acetonitrile and 1% (v/v) acetic acid in acetonitrile were investigated, respectively, and the results are shown in Fig. 3A. It presented that 1% (v/v) acetic acid in acetonitrile as the extraction solvent could achieve higher recoveries. Herein, 1% (v/v) acetic acid in acetonitrile was selected as the extraction agent for further study.

### Optimization of Purification Conditions

The recoveries of analytes at different weights of anhydrous MgSO<sub>4</sub>, DES@MGO, and GCB were investigated at the same concentration (50 µg L<sup>-1</sup> of OCPs) in vegetable matrix extract.

### Optimization of Anhydrous MgSO<sub>4</sub> Weight

Anhydrous MgSO<sub>4</sub> endows a strong water absorption ability and does not react with organic matter, and thus, it was used for removing water from the sample solution. During the experiment, DES@MGO (10 mg) and GCB (1 mg) were used to compare the dewatering effects of anhydrous MgSO<sub>4</sub> (50, 100, 150 mg), as shown in Fig. 3B. The recoveries of δ-HCH were less than 70% which beyond the range of eligible recovery when the amount of anhydrous MgSO<sub>4</sub> was 50 mg or 150 mg. Notably, the recoveries of 5 OCPs were 83–111% with 100 mg of MgSO<sub>4</sub>. Therefore, the anhydrous MgSO<sub>4</sub> weight was set as 100 mg.

**Table 2** Specific surface and pore parameters of MGO and DES@MGO

Sample	BET surface area/ (m <sup>2</sup> g <sup>-1</sup> )	Average pore size/nm	Pore volume/ (cm <sup>3</sup> g <sup>-1</sup> )
MGO	189.74	8.33	0.3953
DES@MGO	178.89	8.00	0.3580

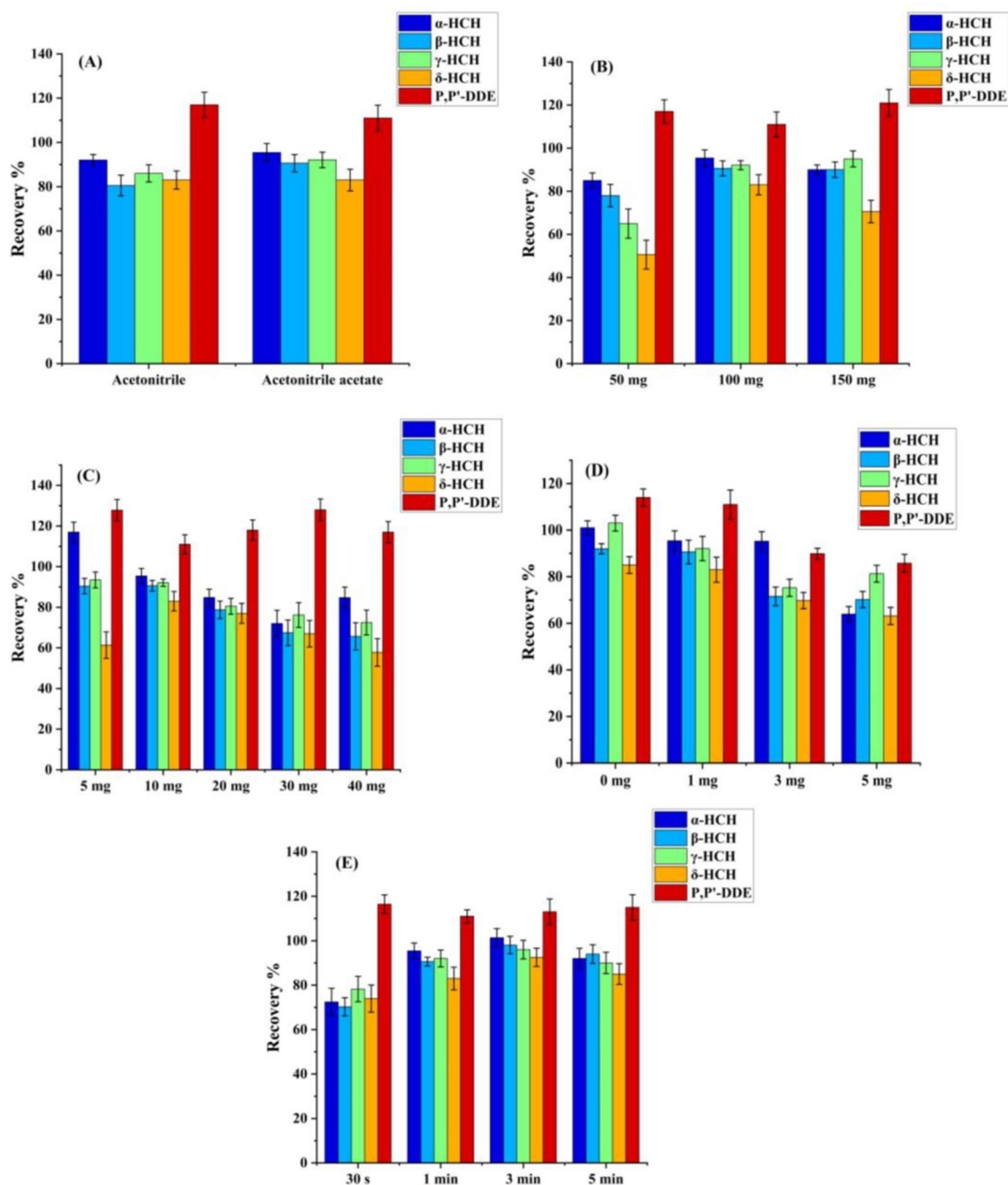


**Fig. 3** Optimization of extraction solvent (A), optimization of anhydrous MgSO<sub>4</sub> weight (B), optimization of DES@MGO weight (C), optimization of GCB weight (D), and optimization of oscillation time (E). Error bars represent standard deviations ( $n=3$ )

### Optimization of DES@MGO Weight

DES@MGO as a new clean-up material achieved a satisfactory recovery. Different weights of DES@MGO (5, 10, 20, 30, and 40 mg) were investigated in the condition of fixing the amount of GCB, as shown in Fig. 3C. When DES@MGO was 5 mg, the recoveries of δ-HCH

were lower than 62% and p,p'-DDE were higher than 125%. When DES@MGO was 10 mg, the recoveries of 5 OCPs ranged from 83 to 111%. While the recoveries of the 5 OCPs decreased obviously when DES@MGO was increased to 20 mg and 30 mg. Except for p,p'-DDE, the recoveries of the other 4 OCPs were below 85%. Therefore, the weight of DES@MGO was selected as 10 mg.



### Optimization of GCB Weight

GCB can remove substances with a planar structure, such as chlorophyll and sterol, from the matrix. Thus, it was selected as the purifier for removing the vegetable pigments. The recoveries of 0, 1, 3, and 5 mg GCB for 5 OCPs were investigated, as shown in Fig. 3D. The results showed that, like the cabbage samples, the extract was light green in color. As can be seen, the pigment could be completely adsorbed and obtained a clear colorless solution with only adding the DES@MGO. For darker vegetables such as spinach, 1 mg of GCB can be added to remove pigment. Moreover, the six-membered ring structure of GCB will adsorb some planar pesticides, so GCB should be avoided for the light-colored sample extract. This was also verified by the recoveries; with the increase of the amount of GCB, the recoveries of 5 OCPs decreased. Herein, GCB was not added.

### Optimization of Oscillation Time

The effects of different oscillation times of 30 s, 1 min, 3 min, and 5 min on the recoveries were investigated, as shown in Fig. 3E. When the oscillation time was 3 min, the recoveries of the 5 OCPs are generally high, so 3 min was selected as the oscillation time.

### Method Validation

The working curves of quantitative ion peak area  $Y$  to the corresponding target concentration  $X$  ( $\mu\text{g kg}^{-1}$ ) for 5 OCPs were plotted by spiking 5.00–100  $\mu\text{g kg}^{-1}$  of each target into vegetable sample of no target pesticides and treating with DES@MGO as QuEChERS clean-up materials. The LODs and LOQs were calculated according to a signal-to-noise ratio of 3 and 10, respectively. As shown in Table 3, all targets have good linear responses with the  $R$  values of from 0.9986 to 0.9997. The LODs range from 0.3 to 2.0  $\mu\text{g kg}^{-1}$ , and the LOQs range from 0.9 to 6.6  $\mu\text{g kg}^{-1}$ .

Recoveries and repeatability were provided by recovery experiments of spiked OCPs in Chinese cabbage matrices at

**Table 4** Standard addition amount, recoveries, and relative standard deviations of five OCPs ( $n=6$ )

Compound	Standard addition amount/ $(\mu\text{g kg}^{-1})$	Recovery/%	RSD/%
$\alpha$ -HCH	10	92.7	5.1
	20	96.1	3.4
	50	102.4	2.6
$\beta$ -HCH	10	85.2	6.7
	20	96.6	4.3
	50	97.4	3.8
$\gamma$ -HCH	10	82.5	7.8
	20	86.1	6.5
	50	95.8	7.2
$\delta$ -HCH	10	97.3	4.8
	20	89.9	6.2
	50	90.1	3.3
$p,p'$ -DDE	10	118.5	6.8
	20	107.2	5.5
	50	111.0	5.6

three different concentration levels (10, 20, and 50  $\mu\text{g kg}^{-1}$ ) with six replicates each. The obtained results are listed in Table 4. The recoveries of 5 OCPs ranged from 82.5 to 118.5% and relative standard deviations (RSDs) ranged from 2.6 to 7.8%, which indicated that the method proposed in this study was of great accuracy, repeatability.

### Comparison of Purification Effect of DES@MGO, PSA, and MGO

The extremely high surface activity of MGO made it to fold and curl and provided a large number of high-energy adsorption sites at its edges and folds. The unbonded  $\pi$  electrons on its surface can form  $\pi$ - $\pi$  interaction with organic molecules, which exhibited good adsorption properties. It can remove pigments, proteins, and organic acid impurities from plant-derived samples. DES has good solubility and a wide polarity range. The DES@MGO produced by the modification of magnetic GO can improve the dispersion and stability of the complex in the matrix, which was

**Table 3** Linear coefficient, ME, detection limit, and quantitative limit

Compound	Matrix curve equation	Linear range/ $(\mu\text{g kg}^{-1})$	Correlation coefficient/ $R^2$	ME	LOD/ $(\mu\text{g kg}^{-1})$	LOQ/ $(\mu\text{g kg}^{-1})$
$\alpha$ -HCH	$y=69.033x+511.9$	5–100	0.9986	13.15%	1.0	3.0
$\beta$ -HCH	$y=38.14x+361.34$	5–100	0.9994	–16.50%	1.0	3.0
$\gamma$ -HCH	$y=56.941x+271.24$	10–100	0.9997	9.63%	2.0	6.6
$\delta$ -HCH	$y=38.668x+63.439$	5–100	0.9995	27.9%	1.0	3.0
$p,p'$ -DDE	$y=193.07x-89.341$	5–100	0.9988	18.82%	0.3	0.9

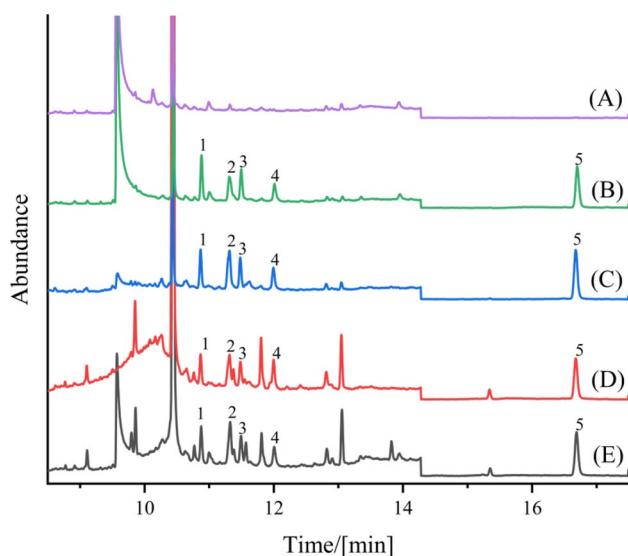


**Fig. 4** Total ion flow chromatography of blank cabbage sample without purification (A), spiked cabbage sample ( $50 \mu\text{g kg}^{-1}$ ) without purification (B), spiked cabbage sample ( $50 \mu\text{g kg}^{-1}$ ) after purification by DES@MGO (C), MGO (D), and PSA (E), respectively.  $\alpha$ -HCH (1),  $\beta$ -HCH (2),  $\gamma$ -HCH (3),  $\delta$ -HCH (4), p,p'-DDE (5)

consistent with the previous characterization results. PSA was an adsorbent similar to the amino group, with two amino groups, which can remove many impurities such as matrix sugars, fatty acids, and organic acids. PSA is a commonly used purifier in the QuEChERS method, which is also used in GB23200.121–2021.

By comparing the chromatograms of the blank sample without purification (Fig. 4A), spiked cabbage sample ( $50 \mu\text{g kg}^{-1}$ ) without purification (Fig. 4B), spiked cabbage sample ( $50 \mu\text{g kg}^{-1}$ ) after purification by DES@MGO (Fig. 4C). It presented that the DES@MGO exhibited a purification effect on the matrix during the sample pretreatment process. On the one hand, it reduced the interference of impurities, improving the detection limit and sensitivity of the target object, along with prolonging the life of the chromatographic column and detector.

To investigate the purification effect of DES@MGO, PSA and MGO on Chinese cabbage sample extract, 5 OCPs ( $50 \mu\text{g kg}^{-1}$ ) were added to blank matrix of Chinese cabbage sample after extraction according to the above method. Then, DES@MGO (10 mg), PSA (25 mg) (refer to GB23200.121–2021), and MGO (10 mg) were used for purification, respectively. Other conditions remained unchanged, and the purification solution was detected by GC–MS, as shown in Fig. 4. It showed many interference peaks in Fig. 4D and E, and the existence of these interference peaks may cause interference to pesticide targets. Particularly, there was an impurity peak in the middle of target 2,3, which caused a serious matrix effect and affected the accurate detection of the two substances. Compared with

Fig. 4C–E presents fewer impurity peaks, and interference in the middle of target 2,3 was also effectively removed. From the chromatogram, it can be seen that target 2,3 has achieved a good separation effect. These results indicated that DES@MGO can affect most of the interfering substances in the acetonitrile extract of Chinese cabbage, and the purification effect was better than PSA and MGO. It could be attributed to the nanoscale porous fold structure of DES@MGO, its large specific surface area and the hydrophobic surface can strongly adsorb disturbances in vegetable samples. After the purification procedure is completed, DES@MGO can be replaced by an external magnetic field to achieve rapid separation of the adsorbent from the solution, simple, and fast. The DES@MGO prepared in this work is an effective purification material with good performance.

## Method Application

Four typical green leafy vegetables (cabbage, spinach, cucumbers, and tomatoes) obtained were analyzed in three replicates. The results showed that the concentrations of all analytes were lower than the LOQs of this method, and lower than  $50 \mu\text{g kg}^{-1}$  standard of maximum residue limit of pesticide (GB 2763–2021).

## Conclusion

In this study, DES@MGO was successfully prepared and characterized, and it was used in QuChERS pretreatment technology, exerting a vital role in good purification effect and rapid magnetic separation advantages. Based on that, DES@MGO was combined with GC–MS to establish the analysis and detection of 5 OCPs in vegetable samples. The results indicated that the average recoveries were 82.5–119%, and the relative standard deviations were 2.6–7.8%. The results showed that the modified QuEChERS method is of simply and rapidity comparing with MGO and PSA. This study provides a reference for the determination of OCPs in vegetables.

**Author contributions** Ling Yu: Investigation, Experimental, Data Curation, Writing-Original Draft, Writing-Review & Editing, Supervision, Funding acquisition. Shujiao Zhang: Investigation, Validation, Formal analysis, Writing-Review & Editing, Supervision. Xu He: Data Curation, Conceptualization, Formal analysis, Writing-Review & Editing. Jie Hu: Methodology, Investigation, Software, Visualization, Data curation. Zhiju Zhao: Conceptualization, Methodology, Investigation, Validation, Formal analysis. Aiqing Xia: Methodology, Investigation, Software, Validation, Formal analysis. Cuijuan Xing: Visualization, Methodology, Investigation, Validation. Ruibing Zhao: Investigation,

Formal analysis, Validation. Jiawei Zhang: Investigation, Formal analysis, Validation. All authors read and approved the final manuscript.

**Funding** This work was supported by Science and Technology Research Project of colleges and universities in Hebei Province, China (QN2023074), key research and development projects in Xingtai, Hebei Province, China, and special project in the field of social development (2022zz049).

## Declarations

**Conflict of interest** The authors declare that they have no competing interests.

## References

- Wang L, Xue C, Zhang YS, Li ZG, Liu C, Pan X, Chen F, Liu Y (2018) Soil aggregate-associated distribution of DDTs and HCHs in farmland and bareland soils in the Danjiangkou Reservoir Area of China. *Environ Pollut* 243:734–742
- Covaciu FD, Floare AV, Magdas DA, David AP, Marincas O (2020) Distribution and fate of persistent organochlorine pesticides on the soil-forage-milk chain in three transylvanian farms. *Anal Lett* 54(1–2):265–279
- Kang YR, Zhang RJ, Yu KF, Han MW, Wang YH, Huang XY, Wang RX, Liu F (2022) First report of organochlorine pesticides (OCPs) in coral tissues and the surrounding airseawater system from the South China sea: distribution, source, and environmental fate. *Chemosphere* 286(P2):131711–131711
- Fang YY, Nie ZQ, Die QQ, Tian YJ, Liu F, He J, Huang QF (2017) Organochlorine pesticides in soil, air and vegetation at and around a contaminated site in southwestern of China: Concentration, transmission and risk evaluation. *Chemosphere* 178:340–349
- Zheng HY, Ding YH, Xue YG, Xiao KY, Zhu JC, Liu YG, Cai MC (2022) Occurrence, seasonal variations, and eco-risk of currently using organochlorine pesticides in surface seawater of the East China Sea and Western Pacific Ocean. *Mar Pollut Bull* 185(Pt A):114300–114300
- Li J, Wang Z, Li JQ, Zhan SH, An YJ, Hao L, Yang XM, Wang C, Wang Z, Wu QH (2022) Novel N-riched covalent organic framework for solid-phase microextraction of organochlorine pesticides in vegetable and fruit samples. *Food Chem* 388:133007–133007
- Wang N, Cui ZW, Wang Y, Zhang JJ (2022) Characteristics and residual health risk of organochlorine pesticides in fresh vegetables in the suburb of Changchun. *Northeast China Int J Environ* 19(19):12547–12547
- Anastassiades M, Mastovská K, Lehotay SJ (2003) Evaluation of analyte protectants to improve gas chromatographic analysis of pesticides. *J Chromatogr A* 1015(1):163–184
- Henrique PM, de Campos BPA, Reyes RFG, Ariseto BAP (2021) Exploring miniaturized sample preparation approaches combined with LCQToFMS for the analysis of sulfonamide antibiotic residues in meat- and/or egg-based baby foods. *Food Chem* 366:130587–130587
- Areo OM, Abafe OA, Gbashi S, Njobeh PB (2023) Detection of multimycotoxins in rooibos and other consumed teas in South Africa by a modified QuEChERS method and ultrahigh performance liquid chromatography tandem mass spectrometry. *Food Chem*. <https://doi.org/10.1016/J.FOODCONT.2022.109255>
- Ma S, Han P, Li A, Wang JH, Feng XY, Wang M (2018) Simultaneous determination of trace levels of 12 steroid hormones in soil using modified QuEChERS extraction followed by ultra performance liquid chromatography-tandem mass spectrometry (UPLC–MS/MS). *Chromatographia* 81(3):435–445
- Temerdashev ZA, Musorina TA, Ovsepyan SK (2022) Determination of polycyclic aromatic hydrocarbons in soils and bottom sediments by gas chromatography-mass spectrometry with QuEChERS sample preparation. *J Anal Chem*. <https://doi.org/10.1134/S1061934822050136>
- Wang J, Duan HL, Fan L, Zhang J, Zhang ZQ (2020) A magnetic fluorinated multi-walled carbon nanotubesbased QuEChERS method for organophosphorus pesticide residues analysis in *Lycium ruthenicum* Murr. *Food Chem* 338:127805–127805
- Yu TX, Wang T, Huang ZL, Huang NS, Zhang H, Luo ZH, Li H, Ding SJ, Feng WL (2017) Determination of multiple pesticides in human blood using modified QuEChERS method with Fe<sub>3</sub>O<sub>4</sub> magnetic nanoparticles and GC–MS. *Chromatographia* 80(1):165–170
- Ma GC, Zhang ML, Zhu L, Chen HP, Liu X, Lu CY (2018) Facile synthesis of amine-functional reduced graphene oxides as modified quick, easy, cheap, effective, rugged and safe adsorbent for multipesticide residues analysis of tea. *J Chromatogr A* 1531:22–31
- Ayyıldız MF, Fındıkoğlu MS, Chormey DS, Bakırdere S (2020) A simple and efficient preconcentration method based on vortex assisted reduced graphene oxide magnetic nanoparticles for the sensitive determination of endocrine disrupting compounds in different water and baby food samples by GC-FID. *J Food Compos Anal* 88(C):103431–103431
- Tan P, Sun J, Hu YY, Zheng F, Qi B, Chen YC, Cheng JH (2015) Adsorption of Cu<sup>2+</sup>, Cd<sup>2+</sup> and Ni<sup>2+</sup> from aqueous single metal solutions on graphene oxide membranes. *J Hazard Mater* 297:251–260
- Song XL, Lv H, Wang DD, Liao KC, Wu YY, Li GM, Chen Y (2022) Graphene oxide composite microspheres as a novel dispersive solid-phase extraction adsorbent of bisphenols prior to their quantitation by HPLC-mass spectrometry. *Microchem J*. <https://doi.org/10.1016/J.MICROC.2021.106920>
- Navid L, Maryam E, Shafiee AM, Khosrou A (2017) Dispersion of magnetic graphene oxide nanoparticles coated with a deep eutectic solvent using ultrasound assistance for preconcentration of methadone in biological and water samples followed by GC-FID and GC–MS. *Anal Bioanal Chem* 409:6113–6121
- Dai YT, Spronsen J, Witkamp GJ, Verpoorte R (2013) Choi YH (2013) Natural deep eutectic solvents as new potential media for green technology. *Anal Chim Acta* 766:61–68
- Borandeh S, Abdolmaleki A, Abolmaleki SS, Tamaddon AM (2018) Synthesis, structural and in-vitro characterization of β-cyclodextrin grafted L-phenylalanine functionalized graphene oxide nanocomposite: a versatile nanocarrier for pH-sensitive doxorubicin delivery. *Carbohydr Polym* 201:151–161
- Abdi G, Alizadeh A, Amirian J, Rezaei S, Sharma G (2019) Polyamine-modified magnetic graphene oxide surface: Feasible adsorbent for removal of dyes. *J Mol Liq* 289:111118
- Wang L, Huang Y, Sun X, Huang HJ, Liu PB, Zong M, Wang Y (2014) Synthesis and microwave absorption enhancement of graphene@Fe<sub>3</sub>O<sub>4</sub>@SiO<sub>2</sub>@NiO nanosheet hierarchical structures. *Nanoscale* 6:3157–3164
- Arash M, Julker NM, Roberto C, Gabriele C, Paolo T, Thanh TT, Dusan L (2020) Graphene oxide (GO) decorated on multi-structured porous titania fabricated by plasma electrolytic oxidation (PEO) for enhanced antibacterial performance. *Mater Design*. <https://doi.org/10.1016/J.MATDES.2020.109443>
- Hosseinazadeh H, Ramin S (2018) Effective removal of copper from aqueous solutions by modified magnetic chitosan/graphene oxide nanocomposites. *Int J Biol Sci* 113:859–868
- Khurana I, Shaw AK, Shaw T, Bharti J, Khurana M, Rai PK (2018) Batch and dynamic adsorption of Eriochrome Black T

- from water on magnetic graphene oxide: Experimental and theoretical studies. *J Environ Chem Eng* 6(1):468–477
27. Mojtaba S, Mehdi F, Mousavi PSA, Hajir K (2022) Tetraethylene-pentamine-enriched magnetic graphene oxide as a novel Cr(VI) removal adsorbent. *React Funct Polym*. <https://doi.org/10.1016/J.REACTFUNCTPOLYM.2022.105410>
28. Marcano Daniela C, Kosynkin Dmitry V, Berlin Jacob M, Sinitskii A, Song ZG, Slesarev A, Alemany Lawrence B, Liu W, Tour James M (2010) Improved synthesis of graphene oxide. *ACS Nano* 4(8):4806–4814
29. Pennante B, David M, SongHee R, GeunHyoung C, SangWon P, ByungSeok K, Hyo KJ, HyoSub L (2021) A comparison of the effectiveness of QuEChERS, FaPEX and a modified QuEChERS method on the determination of organochlorine pesticides in ginseng. *PLoS ONE* 16(1):e0246108–e0246108
- Publisher's Note** Springer Nature remains neutral with regard to jurisdictional claims in published maps and institutional affiliations.
- Springer Nature or its licensor (e.g. a society or other partner) holds exclusive rights to this article under a publishing agreement with the author(s) or other rightsholder(s); author self-archiving of the accepted manuscript version of this article is solely governed by the terms of such publishing agreement and applicable law.